The influence of wind-induced bubbles on echo integration surveys

John Dalen

Institute of Marine Research, Directorate of Fisheries, N-5000, Bergen, Norway

Arne Løvik

Electronics Research Laboratory, The University of Trondheim, The Norwegian Institute of Technology, N-7034 Trondheim-NTH, Norway

(Received 25 August 1980; accepted for publication 25 February 1981)

An investigation of attenuation of acoustic energy caused by gas bubbles in the surface layers has been carried out. This was done primarily to study the effect on echo integration of fish abundance when using hull-mounted transducers. Two different approaches have been used. The first examines the variation of the echo intensity from an acoustically stable bottom layer and the second measures the total volume reverberation as a function of depths. The bubble density, size distribution, and the attenuation caused by the bubbles is estimated from the measurements done under different weather conditions. The results show that the acoustic attenuation caused by wind-induced gas bubbles in the surface layers appear at a lower wind force and at a greater magnitude than earlier reported and expected. The attenuation is found to increase rapidly with increasing frequency. The results are also used to find the minimum towing depths of a transducer as a function of the wind speed necessary in order to keep the attenuation due to the bubbles below a given number.

PACS numbers: 43.30.Bp, 43.30.Gv, 43.30.Dr

INTRODUCTION

During recent decades hydro-acoustic equipment and methods in fisheries research have undergone considerable development up to the present level.[1] Especially within the field of fish stock assessment has the application of scientific echo sounders and echo integration techniques become an excellent tool for fishery researchers.[2] This particular method of abundance estimation is based on the integration of the backscattered sound energy from an aggregation of fish. Utilizing knowledge of the strength of backscattering per individual (i.e., the *in situ* target strength of the individual) or from a known number of fish, the amount of observed fish may be estimated.

Wind- and wave-induced bubbles in the surface layers are known to effect observation by echo sounders.[3] The reason for this is that they will cause excess attenuation of the transmitted and received energy when using transducers located near the surface. A way of overcoming these problems is to use a towed transducer placed under the bubble-occupied water column. Another way is to measure the bubble density, and estimate their size distribution and the attenuation they will cause. The energy loss at transmission and reception may then be compensated for.

In adjacent waters to Norway (i.e., the North Sea, the Norwegian Sea, and the Barents Sea) acoustic surveys are carried out under weather conditions up to wind force Beaufort 7, or 35 kn. When we observe from the echograms and the echo integrator that bubbles in the surface layer are influencing the acoustic observations, we try to correct the integrator recordings by adding a certain value determined on the basis of experience. In relation to our present requirements as to the quality of acoustic observation methods, we find this approach unsatisfactory. Consequently towed transducers are now being increasingly used, but for a long time to come hull-mounted transducers will be in use. For these latter systems we are left with the task of measuring the bubbles and then trying to compensate for their effect on the echo sounding and integrating.

We have found that measuring bubbles in this context can be done by measuring the volume backscattered energy in the upper layers with the same echosounders and transducers as used for fish abundance observations.

Another way of getting information about the excess attenuation from bubbles in the surface layers is by having an integrator-channel working on a bottom layer of constant thickness. Assuming that the acoustic macro-characteristics of this layer undergo just minor and continuous variations within a surveyed area, greater variations of the integrator readings from this layer can be related to changes of the attenuation caused by bubbles in the water column. This will give a quantitative indication of the correction factor to be applied to the echo abundance estimate of fish in the surveyed area.

I. METHODS

A. A simple model for echo integration

For a wide density range,[4] the intensity of an underwater signal scattered back from a collection of scatterers is proportional to the density of the scatterers. This is the basic philosophy for applying echo integration to estimating the abundance of fish stocks. The integration process is illustrated by the block diagram in Fig. 1.

We shall now use the well-known sonar equation to describe the process. The equation is written as

$$\mathrm{EL} = \mathrm{SL} - 2\mathrm{TL} - \mathrm{TL}_b + S + T + E\,, \qquad (1)$$

 0001-4966/81/061653-07$00.80

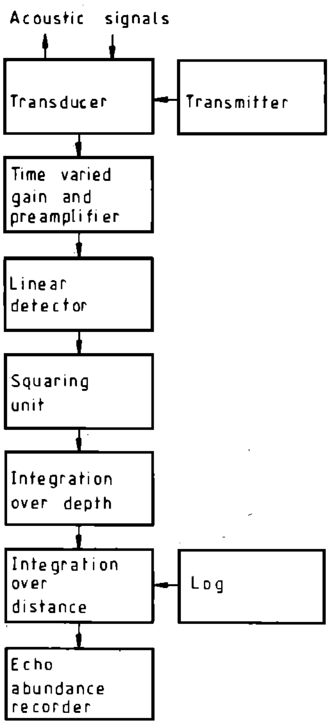

FIG. 1. Block diagram of the echo integration process.

where

EL—echo level representing the backscattered echo intensity of one transmission,

SL—source level representing the output intensity referred to a distance 1 m from the transducer,

2TL—two-way transmission loss consisting of geometrical spreading and acoustic attenuation of the sound energy,

TL_b—two-way transmission loss due to attenuation from bubbles,

S—backscattering strength,

T—$10\log(c\tau/2)$, where c is speed of sound in the medium and τ is transmitted pulse length, and

E—$10\log\psi$ where, ψ is the solid angle of the equivalent beam pattern of the transducer.

The target under consideration is the ocean bottom and we assume that the macro-characteristics of the bottom layer, which we integrate, undergo only minor variations, thus the backscattering strength S is approximately constant. By applying a time varied gain in the receiver and keeping the source level constant Eq. (1) reduces to

$$\mathrm{EL} = \text{constant} - \mathrm{TL}_B\ . \tag{2}$$

The echo abundance is defined as the mean intensity per transmission over a depth interval averaged over a certain distance and corrected for the speed of the vessel. This term is proportional to the echo level, Eq. (2).

B. A model for estimating the density and size distribution of bubbles from volume reverberation measurements

Volume reverberation is described by a volume backscattering coefficient s_v, defined as the backscattering cross section per unit volume. The backscattered sound energy is assumed to add on a power basis. Neglecting the attenuation the reverberation intensity at the transducer, I_r, from a volume V at distance r in the farfield of the transducer is expressed as

$$I_r = \frac{I_0 c\cdot\tau s_v r_r^2}{2r^2}\int_\Omega b_t(\theta,\phi)b_r(\theta,\phi)d\Omega\ , \tag{3}$$

where

I_0—source intensity, W/m^2,

r_r—reference distance m, normally 1 m,

c—speed of sound in the medium m/s,

s_v—volume backscattering coefficient m^{-1},

Ω—solid angle determining the angular coordinates of the observations volume, and

$b_t(\theta,\phi)b_r(\theta,\phi)$—beam pattern directivity functions during transmitting and receiving, respectively. When using stabilized transducers their effect on the observed volume is assumed to be identical and equal to $b(\theta,\phi)$.

The volume V is then given by

$$V = \frac{c\tau r^2}{2}\int_\Omega b^2(\theta,\phi)d\Omega\ . \tag{4}$$

By introducing the equivalent solid angle, ψ, with an intensity I_0 giving the same value of the backscattering as the real directivity diagram, Eq. (3) reduces to

$$I_r = (I_0 c\tau s_v/2r^2)\psi\ . \tag{5}$$

In the nearfield where $r < r_0 = A/\lambda$, the scattering volume, V, is expressed as

$$V = KAc\tau/2\ . \tag{6}$$

K is a constant determined by requiring the nearfield-farfield transition to be continuous, λ is the wavelength, and A is the effective aperture of the transducer.

The intensity in the nearfield, I_{n0}, is assumed to be constant:

$$I_{n0} = I_0(r_r/r_0)^2\ . \tag{7}$$

Continuity of the volume yields

$$K = \frac{A}{\lambda^2}\int_\Omega b^2(\theta,\phi)d\Omega\ . \tag{8}$$

The reverberation intensity from scattering in the nearfield is found by assuming spherical spreading of the scattered field. The intensity at the transducer is then given by Eq. (5). Thus the volume backscattering coefficient can be estimated by measuring the reverberation intensity from a calibrated echo sounder, where I_0 and ψ are known figures, giving

$$s_{vn,f} = (2I_r r^2/I_0 c\tau\psi r_r^2)\ , \tag{9}$$

where the subscripts n,f denote nearfield and farfield, respectively. If the reverberation is due to bubbles, we can estimate the backscattering coefficient as follows:

$$s_v = \frac{1}{4\pi}\int_a \sigma_s(a)n(a)da, \tag{10}$$

where $\sigma_s(a)$ is the cross section of a bubble having a radius a, and $n(a)da$ is the number of bubbles per unit volume. The scattering cross section is

$$\sigma_s(a) = \{4\pi a^2/[(f_0/f)^2 - 1]^2 + \delta^2\}, \tag{11}$$

where f_0 is the resonance frequency of the bubble given by

$$f_0 = (1/2\pi a)(3\gamma P/\rho)^{1/2}, \tag{12}$$

δ—effective damping constant,

γ—ratio of the specific heat capacities of the gas, $\gamma \approx 1.4$.

ρ—density of the water kg/m^3, and

P—ambient pressure Pa.

A first estimate of the integral Eq. (10), is found if it is assumed that the major part of the backscattered sound is from resonant or near-resonant bubbles, i.e.,

$$s_v = N\sigma_s/4\pi, \tag{13}$$

where N is the number per unit volume of "resonant scatterers." From the numbers of resonant bubbles we may deduce the distribution of the bubble density, $n(a)$, by assuming that the scattering around a frequency is from bubbles within the effective bandwidth determined by δ. This gives the bubble density $n(a_0)$ at the resonant bubble radius of a_0 as

$$n(a_0) = N(a_0)/\delta a_0, \tag{14}$$

where $n(a_0)da$ is the number of resonant bubbles per unit volume. In general, using a with the dimension of micrometer, we express the number $n(a)da$ as the number of bubbles in a 1 μm radius interval[5] per unit volume.

At a constant transmitted frequency the radii of the resonant bubbles will vary with depth, $h(m)$, as

$$a_0 = \frac{1}{\omega_0}\left(\frac{3\gamma P}{\rho}\right)^{1/2} = \frac{1}{2\pi f_0}\left[\frac{3\gamma 10^5}{\rho}\left(1 + \frac{h}{10}\right)\right]^{1/2}. \tag{15}$$

The damping constant, δ, is also a function of depth/pressure, and it has a marked frequency dependence. Figure 2 shows how the damping constant varies with the resonance frequency of the bubble. The damping is composed of thermal, viscous, and scattering losses. As seen from Fig. 2, the thermal damping dominates in the frequency region 12–120 kHz. For the determination of the number of scatterers, N, it is assumed that $\delta(h,f) = \delta_{\text{therm}}^{(h,f)}$. When estimating the density distribution, $n(a)$, the effective damping constant is used. This figure is slightly greater than the resonant damping constant.

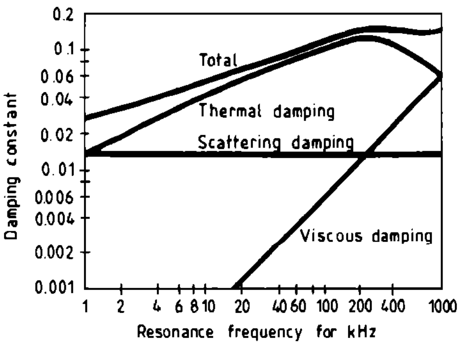

FIG. 2. Damping constant at resonance.

The attenuation rate due to the bubbles, α_b(dB/m) is estimated by using the following expression,

$$\alpha_b = 4,34\, N\sigma_e, \tag{16}$$

where σ_e is the extinction cross section of a bubble and is given by

$$\sigma_e = \frac{4\pi a^2\,\delta/\delta_s}{[(f_0/f)^2 - 1]^2 + \delta^2}, \tag{17}$$

with δ_s being the damping caused by scattering at resonance. As we often experience high wind velocities it is likely that there will be a large number of bubbles in the upper water column. The corresponding attenuation of the sound wave per unit distance caused by multiple scattering is then of great importance and must be included. In the following we shall look at the effect of taking the attenuation caused by the bubbles into account. A solution will be sketched for the case when the attenuation, α_b, is small, which will also serve to illustrate the effect on the estimate of the number of bubbles. This approximation is especially useful when the ratio of the extinction and backscattering cross section is large, i.e., $\sigma_e/\sigma_s \gg 1$, which is the case for resonant gas bubbles.

The reverberation intensity, I_r, Eq. (5) hence becomes

$$I_r = \frac{I_0 c\tau s_v \psi r_r^2}{2r^2}\exp\left(-2\int_0^r \alpha(r)dr\right). \tag{18}$$

By inserting the expressions for s_v and $\alpha(r)$ in Eqs. (9) and (16), this can be re-arranged to

$$N\exp\left(-2\int_0^r N\sigma_e dr\right) = N_0(r), \tag{19}$$

where

$$N_0(r) = (8\pi r^2 I_r/c\tau\psi\sigma_s I_0 r_r^2), \tag{20}$$

which gives the number of resonant bubbles in absence of multiple scattering. Differentiating Eq. (19) with respect to r and multiplying this by N_0 yields

$$N' - NN_0'/N_0 - 2N^2\sigma_e = 0. \tag{21}$$

This is a Bernoulli equation, the general solution of which can be written as

$$N(r) = 1/z(r), \tag{22}$$

where

$$z(r) = \exp\left(-\int_0^r \frac{N_0'}{N_0}dr\right)\left\{C - \int_0^r\left[2\sigma_e\Big/\exp\left(-\int_0^r \frac{N_0'}{N_0}dr\right)\right]dr\right\} \tag{23}$$

and C is a constant. The measurements show that

$$N_0 \sim n_0\exp(-kr), \tag{24}$$

where the bubble density at the reference depth, d_0, is in $n_0(d_0)$, and k is a coefficient determining the decrement of N_0 for increasing r.

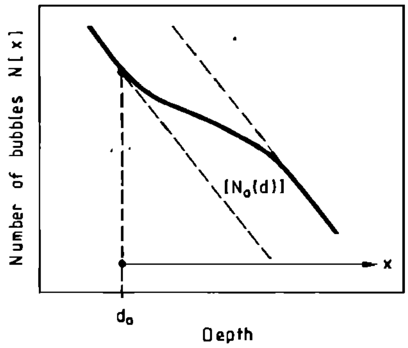

FIG. 3. Number of bubbles per unit volume versus depth.

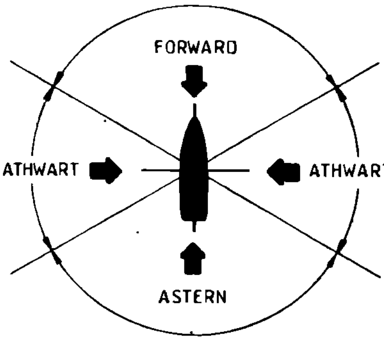

FIG. 5. Sectors of wind directions relative to the vessel.

By applying this form of N_0, and, as an example, assuming that the extinction cross section is constant, the number of bubbles $N(r)$ can be found. C is determined by requiring that $N(x) = n_0(d_0) = n_0$ for $x = 0$. The solution of Eq. (21) will then be

$$N(x) = \left[n_0 \exp(-kx) \Big/ \left(1 - \frac{2\sigma_e n_0}{k}[1 + \exp(-kx)]\right)\right]. \tag{25}$$

For large values of x we have

$$N(x) = \left[n_0 \exp(-kx) \Big/ \left(1 - \frac{2\sigma_e n_0}{k}\right)\right]. \tag{26}$$

The solution is shown diagrammatically in Fig. 3.

From Eq. (26) and Fig. 3 we see that neglecting the attenuation of the incoming and scattered wave leads to an underestimate of the number of bubbles, which is quite reasonable from a physical point of view.

II. THE MEASUREMENTS

A. Integration of a bottom layer

During a survey on demersal fish in the Barents Sea in the winter of 1977 a pilot study was carried out to elucidate the effect on echo integration of fish from wind- and wave-induced bubbles in the surface layers. This was done by integrating a bottom layer of approximately constant thickness, and looking for variations due to weather changes. The bottom channel was chosen to be 10 m, see Fig. 4. The equipment used was SIMRAD EK 38 echo sounder, sounding at 38 kHz, and a SIMRAD QMMK II integrator. Simultaneous data of wind force, wind direction, and of course speed of the vessel were recorded. The bottom channel contained both fish and part of the seabed. The contribution from the seabed was found to be on average 10^4 times greater than that from the fish. From this result we may conclude that the integrator recordings of the bottom channel are from the seabed only.

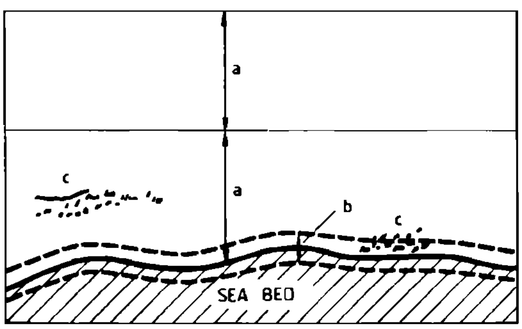

FIG. 4. Echogram showing the integrator intervals. a—fish integration intervals, b—bottom integration interval, and c—fish recordings.

Wind and waves will influence the motion of a vessel in different ways depending on the relative course and speed of the vessel and the wind and waves. This in turn will lead to different variance or spread of the integrator recordings from the bottom channel. The total horizontal plane is therefore divided into four sectors, as shown in Fig. 5, where the course of the vessel relative to the direction of the wind and waves is indicated.

For wind forces exceeding 20 to 25 kn head-on the speed of the vessel was reduced to 6–8 kn, otherwise normal cruising speeds of 9 to 12 kn were maintained as long as the wind force did not exceed 35 to 40 kn.

The reference value of the echo abundance (Figs. 6 and 7) corresponding to 0–dB reduction is an arbitrary one corresponding to a wind force producing an excess absorption which yields approximately a 10% reduction of the received echo intensity. This is calculated and read from Fig. 12 for 38 kHz.

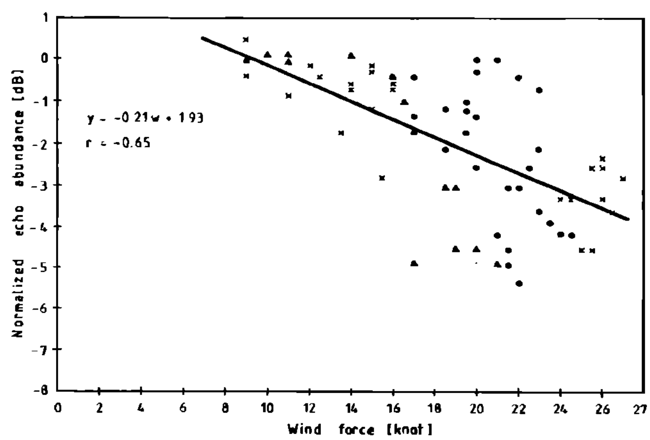

FIG. 6. Normalized echo abundance versus wind force for wind direction from; o—forward, Δ—athwart, and ×—astern. The drawn line $y = 0.2W + 1.93$ is the linear regression estimate, with a regression coefficient $r \sim 0.65$.

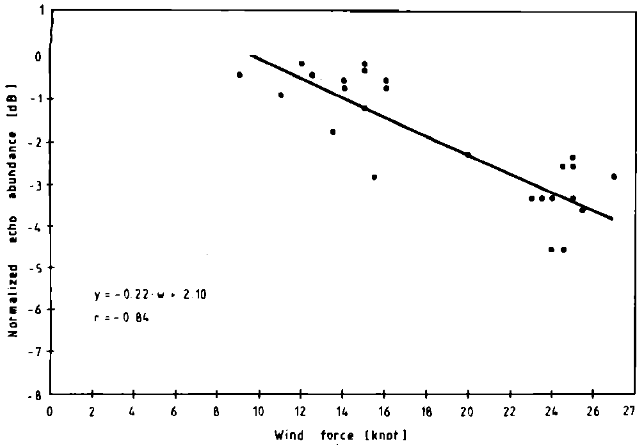

FIG. 7. Normalized echo abundance versus wind force for wind from astern. The drawn line $y = 0.22W + 2.10$ is the linear regression estimate with a regression coefficient $r \sim 0.84$.

B. Measurement of the volume reverberation

The measurements were carried out during two surveys in 1978 by applying the scientific echo sounders SIMRAD EK at 12, 38, and 120 kHz. The received signal was taken out of the receiver just after the transmit/receive switch. The instrument setup is shown in Fig. 8. Stabilized transducers were used.

The reverberation level was analyzed as a function of depth with a resolution in depth of 0.45 m. At each depth the applied result is approximately 3 dB over the mean value of the reverberation. The transducers were assumed to be at a stable depth of 5 m for all wind forces.

III. ESTIMATION OF THE DENSITY AND DISTRIBUTION OF BUBBLES

Figure 9 shows the measured resonant bubble density at 38 kHz as a function of depth for different wind forces. The wind force is the average value over 10 min. The results at 12 and 120 kHz show the same trends with respect to wind force and depth dependences.[6]

All the measured values tended to flatten out at greater depths. This level corresponds to the received noise level in the measuring system rather than to a physical feature of the bubble distributions.

Figure 10 shows the bubble density at 8 m versus wind force, read at 38 kHz. Data from adjacent depths produced lines parallel to that of Fig. 10.

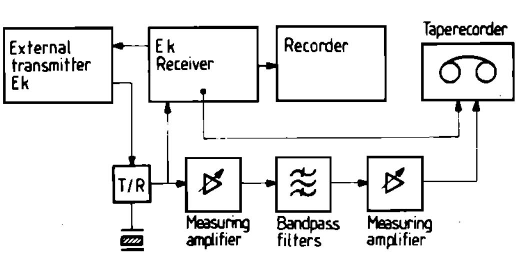

FIG. 8. Instrument setup.

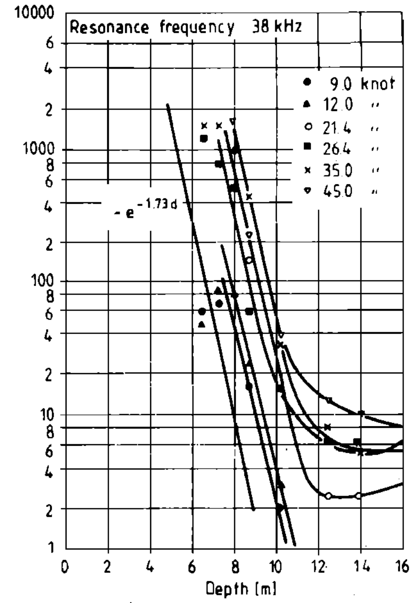

FIG. 9. Resonant bubble density at 38 kHz versus depth.

IV. DISCUSSION

To elucidate the effect of the excess attenuation of the received sound energy when doing echo integration, we consider Eq. (2). We see here that any observable variation of the total attenuation from bubbles will appear as variations of the echo intensity which relates to the respective echo abundance.

Both Figs. 6 and 7 show the trend of the reduction of the echo abundance with increasing wind force. Greater variations are observed when the wind is from both the forward and athwart directions relative to the course of the vessel than from astern only. If we look for a figure to correct the observed echo abundance from fish under different wind conditions from observations like this, the data obtained when the wind came from astern should

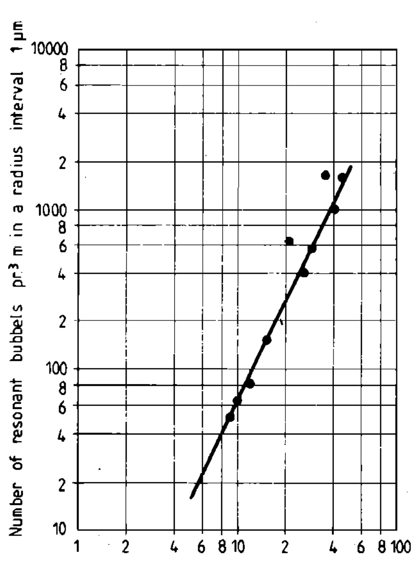

FIG. 10. Bubble density versus wind force at 8 m. Resonance frequency 38 kHz.

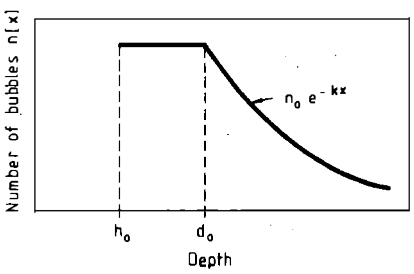

FIG. 11. Assumed number of bubbles as a function of depth.

be recommended. This situation corresponds to the vessel being as stable as possible, thus keeping the influence of the motion of the vessel to a minimum.

By measuring the volume reverberation on an echo sounder and applying the simple theory of volume scattering, we have estimated the number of resonant gas bubbles and the excess attenuation they cause at different wind forces. Detailed information about these observations is given in Ref. 6.

The total excess attenuation can be found from the following equation:

$$A_{tb} = 8,68 \int_{h_0}^{r_1} \sigma_e N(r) dr \,, \qquad (27)$$

where the depth of the transducer, h_0, is 5 m and r_1 is the range of the target. To solve this integral we assume that the thermal damping is dominant, see Eq. (18), and that the number of bubbles varies with depth as shown in Fig. 11. The depth d_0 is determined from the measurements as the minimum detection depth and is put equal to 8 m at 38 kHz.

The results are presented in Fig. 12 for the three frequencies, when the range of the target r_1 is at infinity. We see that the attenuation from bubbles increases rapidly with increasing frequency. This should,

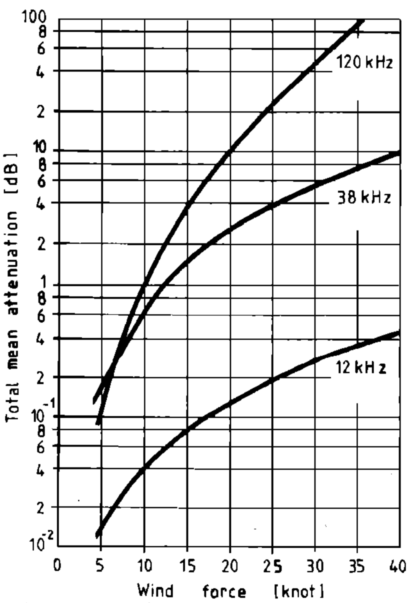

FIG. 12. Total attenuation versus wind force at 12, 38, and 120 kHz.

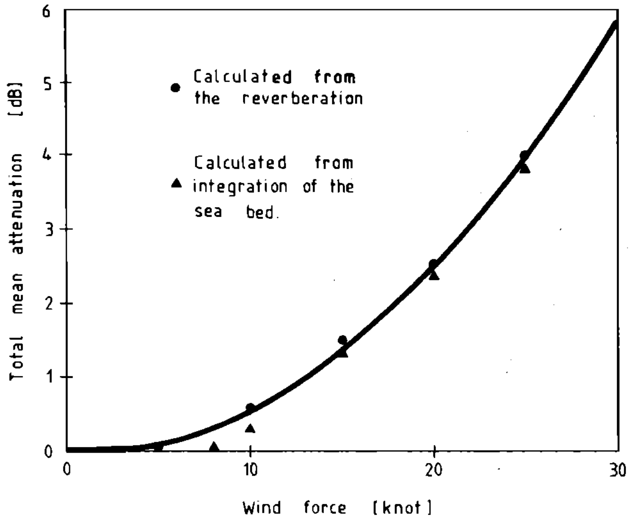

FIG. 13. Total mean attenuation versus wind force at 38 kHz, based on the reverberation (●) and the echo integration data (▲).

for instance, remind everyone using high-frequency echo sounders for quantitative measurement of fish abundance to be aware of this particular source of error in their abundance estimate.

How are the results from the volume reverberation measurements at 38 kHz in accordance with the integrator measurements of a bottom layer? Figure 13 shows the calculated excess attenuation caused by the gas bubbles together with the data obtained from integration of the seabed. The results from these two different and independent methods of calculation and measurement agree very well over the common range of wind velocities.

The measured bubble densities may also be used to find a minimum towing depth for a towed body as a function of wind velocity in order to maintain a given attenuation caused by the bubbles. If we assume that the bubble layer follows the movement of the sea surface the minimum depth is taken as the sum of the bubble

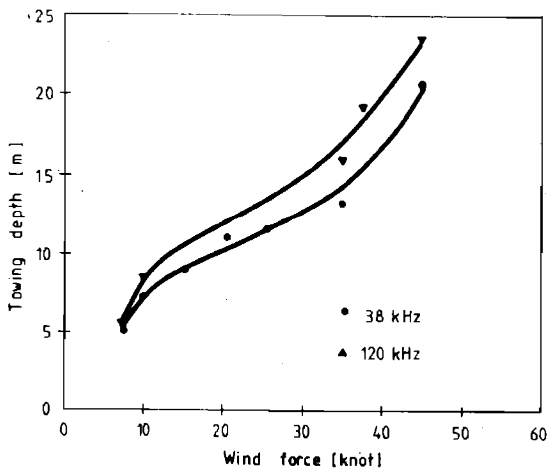

FIG. 14. Minimum towing depth as a function of wind force to give a bubble attenuation less than 0.3 dB.

layer and the wave height. The wave height h is found from Schulkin and Shaffer's formula written as[7]

$$h = 0.0008\ V^{5/2}\ ,$$

where h is the crest-to-trough wave height in meters and V is the wind speed in knots.

The thickness of the bubble layer is found by calculating the depth which gives an attenuation of only 0.3 dB. The results are shown in Fig. 14 for the two frequencies 38 and 120 kHz, as the minimum towing depth as a function of wind force giving an attenuation caused by gas bubbles of 0.3 dB. As expected the necessary depth is greater for the highest frequency.

To our knowledge, the used towing depths for fish abundance estimation varies from 3 m and downwards. Clearly this range of depth covers the entire depth variation as shown in Fig. 14 and the users of small towing depths should be aware of the possible errors due to the bubble layer.

V. CONCLUSIONS

Two methods of studying the attenuation caused by air bubbles in the sea are presented. One method is based on echo integration and the other on measuring the volume reverberation.

The echo integration observations done at 38 kHz show that the echo abundance from a stable bottom layer decreases with increasing wind force.

The bubble measurements done at 12, 38, and 120 kHz show that the total attenuation through the bubble layer is greatest at 120 kHz and lowest at 12 kHz. At 38 kHz, which is an often used frequency on research vessels, a wind force of 20 kn will be responsible for an excess transmission loss of approximately 2.5 dB.

The results from the two different surveys give excellent agreement.

A graph is given showing the minimum towing depth as a function of wind force necessary if the attenuation due to bubbles is to be less than 0.3 dB.

Before establishing any figure to correct the observed echo abundance from fish under different wind conditions, the two kinds of measurements should be run simultaneously. To reduce some of the influence from the motion of the vessel the pitch and roll should be monitored and fed back during the analysis of all the collected data.

ACKNOWLEDGMENTS

The authors are indepted to K. Hansen and I. Svellingen and their coworkers of the instrument staff on board R. V. "G. O. SARS" for enthusiastic assistance during the data aquisition periods and to A. Raknes and Å. Kristensen for data scrutinizing and processing.

[1] *Manual of methods for fisheries resource survey and appraisal. Part 2. The use of acoustic instruments for fish detection and abundance estimation*, edited by S. T. Forbes and O. Nakken (FAO, Rome, 1972).

[2] J. Burczynski, "Introduction to the use of sonar systems for estimating fish biomass," FAO Fish. Tech. Pap. 191, FIRM/T191 (1979).

[3] H. Medwin, "Acoustic fluctuations due to microbubbles in the near-surface ocean," J. Acoust. Soc. Am. 56, 1100–1104 (1974).

[4] I. Røttingen, "On the relation between echo intensity and fish density," Fiskerdir. Skr. Ser. Havunders. 16, 301–314 (1976).

[5] H. Medwin, "In situ acoustic measurements of bubble populations in coastal ocean waters," J. Geophys. Res. 75 (3) 599–611 (1970).

[6] A. Løvik, "Acoustic measurements of the gas bubble spectrum in water," in *Cavitation and inhomogeneities in underwater acoustics*, edited by W. Lauterborn (Springer–Verlag, Berlin, 1980).

[7] R. J. Urick, *Principles of Underwater Sound* (McGraw–Hill, New York, 1975), pp. 242.